Eur J Cancer Clin Oncol, Vol. 21, No. 3, pp. 379–387, 1985.
Printed in Great Britain.

0277-5379/85$3.00+0.00


# Nuclear Magnetic Resonance (NMR) Proton Imaging in Cancer

FRANCIS W. SMITH
*Aberdeen Royal Infirmary, Fosterhill, Aberdeen AB9 2ZB, U.K.*

## INTRODUCTION

WITHIN 10 yr of the introduction of X-ray computed tomography (X-ray CT), diagnostic radiology has found itself on the threshold of a second revolution in imaging technique. The development of nuclear magnetic resonance (NMR) for imaging now enables the diagnostician to not only see normal anatomy and gross pathological change, but to study organ function and pathophysiologic change *in vivo*.

A great deal of interest in the technique has been generated, because of its ability to produce high-resolution images of areas which hitherto have been difficult to image, such as the posterior fossa, brain stem and neck (Fig. 2), because of its ability to demonstrate blood vessels without the use of contrast agents (Fig. 3) and because tumours show very clearly, again without the use of contrast (Fig. 4). However, much basic clinical research into its true place in diagnosis has yet to be performed. This paper attempts to describe in simple terms the NMR phenomenon and how it is applied for imaging. It also describes some of the work which has been performed at the Aberdeen Royal Infirmary over the past 4 yr to find its place in cancer diagnosis and management.

## PHYSICAL PRINCIPLES

The NMR phenomenon and the methods used for obtaining images with it are quite complex. Some of the phenomena can be explained only by quantum mechanics, but those relevant to a basic comprehension of the technique and sufficient for the appreciation of its applications in medicine may be understood using the principles of mechanics and magnetism.

To understand the underlying phenomenon, we should return to basic physics and chemistry. Each atomic nucleus is made up of nucleons, that is, protons and neutrons (the one exception to this is the hydrogen atom, which consists of a single proton). These nucleons rotate or 'spin' about their axes. When pairs of protons or pairs of neutrons exist in the nucleus, they align in such a way that their spins cancel each other out, and such pairs are of no interest to us for this discussion. However, when a nucleus contains an unpaired proton or neutron or both, the nucleus will have a net spin (i.e. it will rotate on its axis). Because the nucleus has an electric charge, the spin corresponds to a current flowing about the spin axis; this in turn generates a magnetic field. The nucleus may, therefore, be considered a small bar magnet spinning on its axis.

In normal circumstances, these nuclei spin while pointing in a random direction, but when placed in a uniform static magnetic field, a portion of them will align with the field's lines of force. These spinning nuclei behave like tiny spinning tops or gyroscopes which, if tipped away from the vertical axis, will rotate about this axis in a motion known as 'precession'. To make the nuclei precess around their axes, a smaller external electromagnetic field must be applied. This applied electromagnetic radiation must match the natural precessional frequency of the nuclei in the sample, hence the term nuclear magnetic resonance. This resonance frequency, often known as the Larmor frequency, is related mathematically to the externally applied magnetic field. The frequency is equal to the strength of the field measured in tesla (T; 1 tesla = 10,000 gauss) multiplied by the gyromagnetic frequency, which is unique for each species of nucleus. Thus, for hydrogen protons in a 1-tesla field, the resonance frequency is 42.57 MHz. In the same field, the resonance frequencies of $^{31}P$ and $^{23}Na$ are 17.24 and 11.26 MHz respectively. These frequencies are far below those of X-rays and visible light, and are too weak to do any biological damage.

By choosing relevant frequencies, one can tune in to specific nuclei and observe their reactions. So

Accepted 19 September 1984.

far, all medical NMR images have been obtained with resonances from hydrogen nuclei ($^1H$). This is because hydrogen is not only abundant in the body, but also has a higher intrinsic NMR sensitivity than do other nuclei. $^{31}P$ is found in concentrations too low to image at present, but it is in sufficient quantity to be measured spectroscopically.

Several methods are available that use the NMR signal for image production. By manipulation of smaller electromagnetic fields around the static field, a number of different imaging techniques have been developed. Whether they use the projection reconstruction method used in X-ray CT or the sensitive-point, sensitive-line, steady-state free precession or spinwarp methods, they all rely on measuring proton density and proton-relaxation times ($T_1$ and $T_2$). Each of the different methods produces a slightly different type of image. Some are pure proton density and others are pure $T_1$, whereas still others are a combination of proton density, $T_1$ and $T_2$.

The different methods all rely on pulsed radio-frequency radiations of known strength, but they vary in the length of the pulse applied to manipulate the protons. The pulse sequence may also be varied (i.e. the intervals between pulses may be varied) to obtain useful data for image construction. The principles of the image production are simply explained. When the length of the applied radio frequency is increased (so that the angle of precession is rotated through 90° and then stopped), the protons decay or relax, emitting the radiation they absorbed when they moved through 90°. The strength of this signal is a measure of the proton density of the section being examined. If a longer excitation pulse is used, the angle of precession can be moved through 180° (i.e. the spins are inverted). When the radiation is measured (specifically, the length of time taken for the protons to return to equilibrium), the proton spin-lattice relaxation time or $T_1$ is measured. $T_1$ varies from substance to substance, this variation depending on the relationship of the hydrogen atoms to their surroundings or molecular lattice. Short relaxation times exist where water (rich in hydrogen) is closely bound to proteins such as are found in muscle or liver, or in fat, which is also rich in hydrogen. Long relaxation times occur in fluids such as urine and cerebrospinal fluid. Depending on the amounts of free and bound water in tissues, the $T_1$ will vary, allowing for good tissue discrimination and evaluation. The other important relaxation time is $T_2$, or the spin-spin relaxation time. Its magnitude depends on the magnetic interaction between nuclear spins during the relaxation or decay period. It therefore makes a significant contribution to the decay of the NMR signal. It may be measured specifically by applying a string of 180° pulses and recording the decaying emitted signal. As mentioned earlier, a number of different types of image may be produced. Proton density may be displayed as a pure calculated proton-density map or used as the major signal in saturation recovery images. $T_1$ may similarly be displayed as a pure calculated value or as the major component of inversion recovery images. $T_2$ measurement is used as the main constituent of spin-echo images. The foregoing description is, of necessity, simple; for a more detailed but nonetheless basic description, a number of articles may be consulted [1, 2].

## IMAGING METHOD

The NMR imager built in Aberdeen by Dr James Hutchison and his team under the direction of Prof. John Mallard has been in clinical use since August 1980. Since this time over 2000 patients and normal volunteers have been examined with no ill effects.

The Aberdeen NMR imager uses a low field strength resistive magnet of 0.08 T (800 G) which produces a resultant frequency of 3.4 MHz for the hydrogen proton. The 'spin-warp' method of imaging is used; this method is not described since it is beyond the scope of this paper and is well described elsewhere [3–5]. The data to produce each set of images of a section are collected in just over 4 min (256 sec); each section may be either 1.2 or 1.5 cm thick.

The image data are collected on a 128 × 128 matrix and interpolated to a 256 × 256 display. Each image is displayed in grey-scale.

## CLINICAL EXPERIENCE

*Brain*

NMR imaging can clearly differentiate white from grey matter in the brain. The grey matter has about 14% more water than white matter, which means it has a longer proton relaxation time, making for a considerable contrast between the two.

Over 500 cases of suspected central nervous system lesion have been examined and the majority have been compared with X-ray CT. We have shown that, because of their long relaxation times, all intracranial tumours can be demonstrated clearly. Unfortunately cerebral oedema also has a long relaxation time and it is often difficult to differentiate the tumour/oedema interface. This is not considered to be a major drawback since, in all cases of cerebral tumour, the tumours have been more clearly demonstrated by NMR than by CT. Another difference between NMR and X-ray CT is that NMR does not

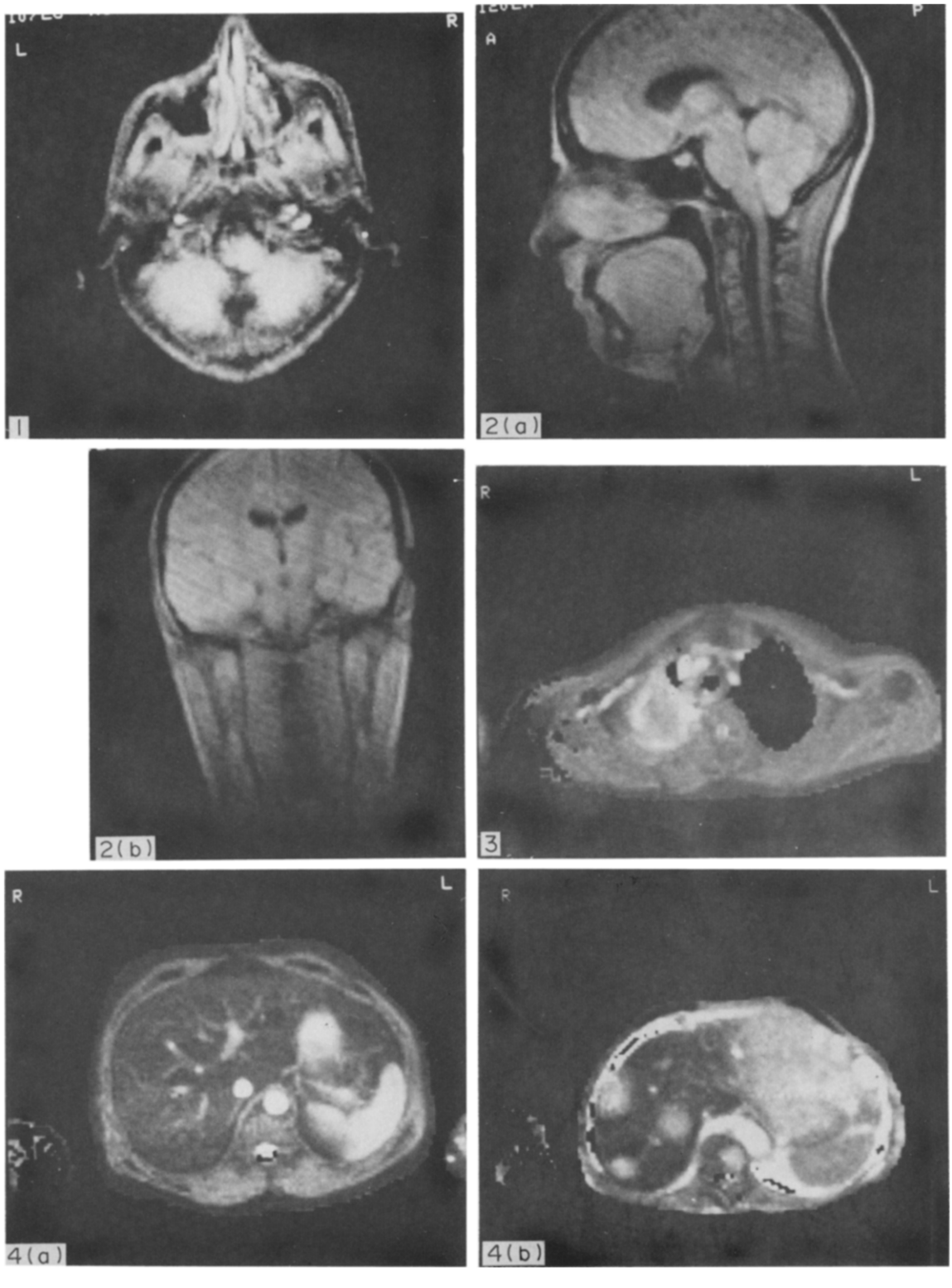


*Fig. 1. Axial section. Glioma situated in the right side of the medulla. It appears white and indents the fourth ventricle.*

*Fig. 2. (a) Midline sagittal section, head and neck in a patient with an Arnold-Chiari malformation. Note the excellent demonstration of the pituitary gland, optic chiasma, brain stem, cerebellum and cervical cord. The nasal turbinates, tongue and epiglottis are also well demonstrated. (b) Coronal section of brain and neck showing normal ventricular system and carotid arteries (black).*

*Fig. 3. Pancoast tumour, right apex. Major blood vessels appear white. The tumour is grey and is surrounded by an effusion (white).*

*Fig. 4. (a) Normal liver. (b) Liver containing metastases from ovarian carcinoma. Note the ascitic fluid (white) and the metastasis in the vertebral body.*

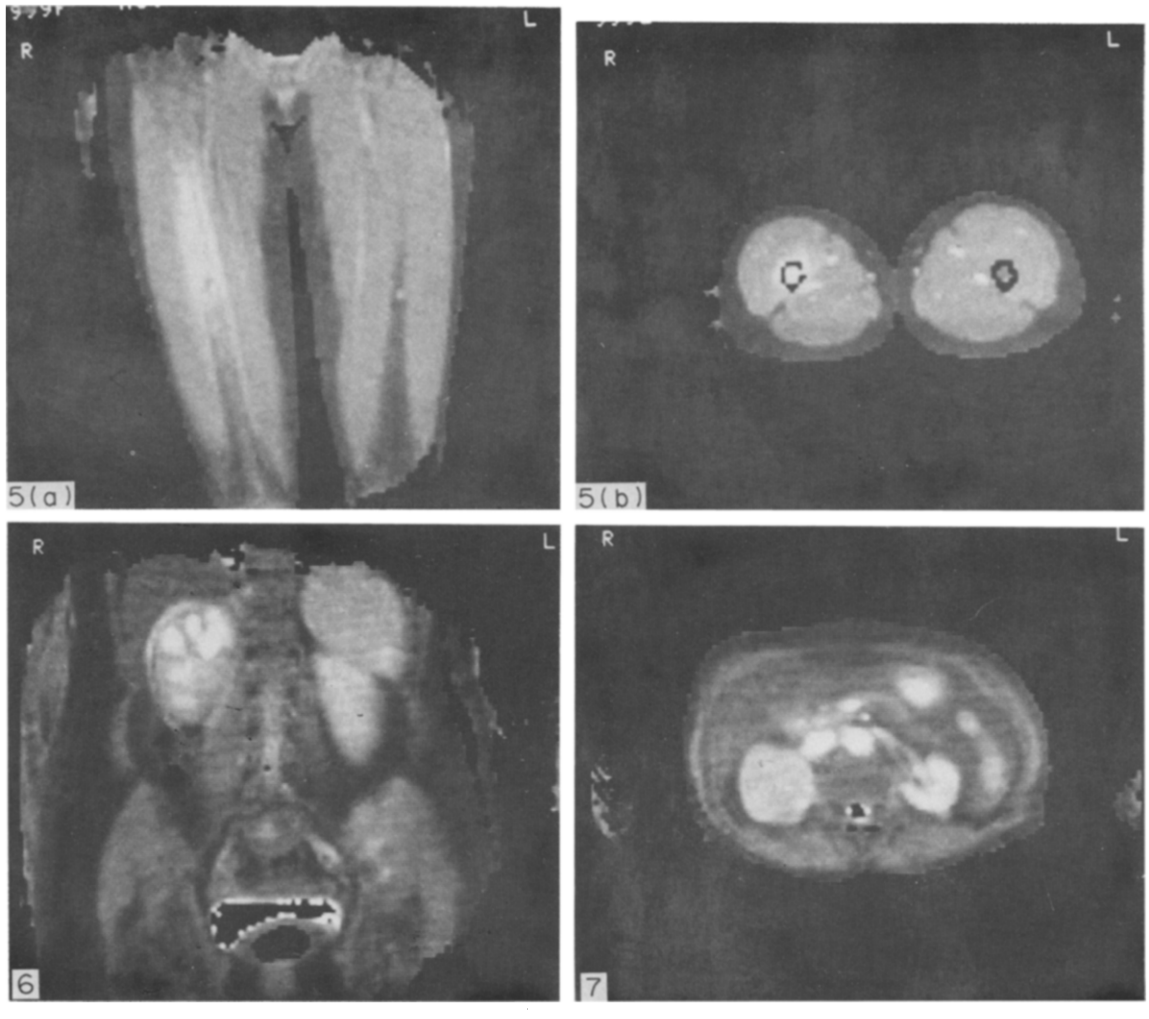


*Fig. 5. (a) Coronal; (b) axial. Ewing's sarcoma in right femur. The tumour is seen as white in the marrow cavity and soft tissues surrounding the bone. The normal left femur has a grey marrow cavity. In both, the cortical bone appears black.*

*Fig. 6. Coronal section demonstrating transitional cell carcinoma in the renal pelvis of the right kidney and resultant calyceal dilatation.*

*Fig. 7. Axial section. Renal cell carcinoma of the right kidney.*

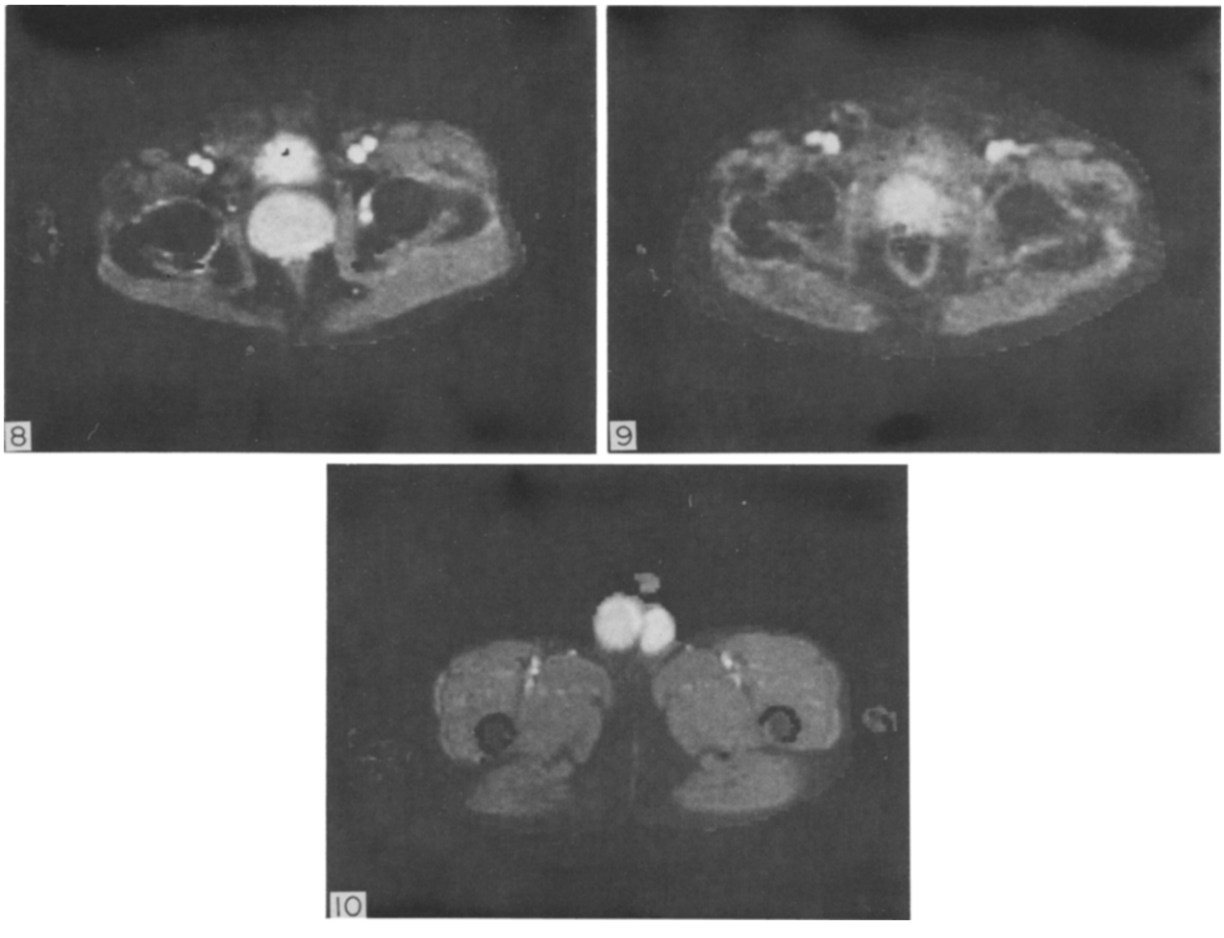


*Fig. 8. Axial section showing benign prostatic hypertrophy.*

*Fig. 9. Axial section showing carcinoma of the prostate. The tumour is infiltrating through the capsule, giving it an irregular outline, in contrast to the well-encapsulated gland shown in Fig. 8.*

*Fig. 10. Axial section. Teratoma in the right testis. The tumour appears grey, having a shorter relaxation time than the normal left testis.*

demonstrate calcification within tumours. This also is not a major disadvantage because the presence or absence of calcium in a tumour does not alter the prime diagnosis, it only influences the differential diagnosis. We believe that NMR has very little to add to diagnosis of cerebral lesions over X-ray CT.

NMR is superior to X-ray CT in demonstrating tumours of the brain stem and cerebellum (Fig. 1) due to the absence of artefact and attenuation of the signal by the petrous bones that occurs with X-ray CT. The ability to produce primary sagittal and coronal sections of this 'difficult' area means that NMR can contribute significantly to the diagnosis and managment of posterior fossa tumours (Fig. 2).

*Head and neck*

When examination of the paranasal sinuses, nasopharynx and orbits are made with NMR no bone or air artefacts which are seen with X-ray CT are seen, and tumours of the head and neck are readily seen.

By demonstrating the long relaxation time of malignant tissue NMR can identify malignant involvement of cervical lymph nodes, even in the absence of nodal enlargement. However, because inflammatory tissue also has a long relaxation time, differentiation of inflammed nodes and those showing reactive hyperplasia from malignancy may be difficult.

The use of sagittal imaging in the assessment of nasopharyngeal and laryngeal tumours allows for precise delineation of tumour extent for radiotherapy planning.

*Thorax*

The ability to differentiate between benign and malignant breast tumours has been shown to be possible in large masses, but before NMR can be advocated as a method for 'breast screening' very large series of patients must be studied and its ability to demonstrate tumours less than 0.5 cm in diameter proven.

In the thorax one of the most striking features of proton images is their ability to demonstrate blood vessels without added contrast media. This ability allows for accurate diagnosis of mediastinal masses and may be used to differentiate vascular anomalies from tumour when opacities are seen on plain X-rays, and also for the full extent of tumour involvement in the mediastinum to be made (Fig. 3).

Small primary and secondary tumours in the lung, less than 1.0 cm in diameter, may not always be demonstrated due to respiratory motion moving the mass in and out of the section during imaging. Until either respiratory gating to control image acquisition or shorter imaging times are developed, X-ray CT is considered to be more reliable than NMR for the diagnosis of small peripheral lung lesions. However, NMR is considered to be more suitable for demonstrating the extent of mediastinal tumour.

*Bone*

When NMR was first applied to body imaging, it was thought that because of the weak or absent signal from cortical bone, it would be of no value in the demonstration of bone disease. This is not the case, since all tumour involvement of bone also involves the bone marrow and the presence of malignant tissue with a long relaxation time is clearly seen in the marrow (Figs 4 and 5) and also in the adjacent soft tissues when the tumour spreads into them (Fig. 5).

It is most unlikely that NMR will replace radionuclide bone scanning for the demonstration of bone secondaries, but it may provide a method for monitoring their response to treatment.

*Liver and pancreas*

Early work with NMR imaging showed that it was both more specific and more sensitive than either ultrasound or radionuclide scan in the diagnosis of a wide spectrum of hepatic disease [9–11]. Recent work has shown that, because of the greater contrast between normal and abnormal liver tissue, NMR is probably as accurate as CT scanning in the diagnosis of liver disease.

Using the Aberdeen NMR imager, we have shown that the presence of fat in early hepatic disease, iron in haemochromatosis or copper in Wilson's disease leads to a shortening of the relaxation time, while the presence of inflammatory cells and oedema in hepatitis and cirrhosis leads to an increase. The abnormal pattern in these conditions tends to radiate out in a reticular pattern from the portal tracts.

There is some overlap of relaxation times for cirrhosis and both primary and secondary tumours, but the pattern and distribution of the lesions usually facilitate differentiation. Benign lesions, such as haemangiomas, are easily distinguished from malignant tumours by the measurement of relaxation time, the blood within the masses giving characteristic values. While some necrotic tumours and abscesses may have $T_1$ values in the same range as blood, with care it is possible to interpret the images correctly.

In a study at the Aberdeen Royal Infirmary the response of hepatic secondaries to chemotherapy is being followed by NMR imaging. Although it is too soon to draw definite conclusions, preliminary findings indicate that NMR is a sensitive method of demonstrating early tumour

regrowth. In one patient with hepatic metastases from seminoma, who was receiving chemotherapy, the secondaries were seen to regress and, as they did, the level of specific tumour marker in the blood fell to normal. For 2 months the liver images appeared to be normal but, at the beginning of the third month, an irregular area of $T_1$ was seen in the left lobe of the liver (where the largest of the secondary tumours had been), even though the level of tumour marker in the blood still remained normal. Two weeks later the marker levels were elevated and NMR images showed a massive tumour in the left lobe and further deposits in the right. Since NMR had demonstrated the recurrence of the tumour before other methods, it suggests that it has potential for tumour growth monitoring.

Our preliminary studies indicate that NMR may prove more reliable than either ultrasound or CT scanning in the demonstration of pancreatic disease. The ability to detect areas of different $T_1$ value, coupled with the absence of artefact from bowel gas, peristalsis and bone, make NMR ideal for the examination of pancreas and other retroperitoneal tissue. Normal pancreas is not always seen easily because of its similarity in relaxation time to the surrounding tissue, but it can be localized by its relationship to the superior mesenteric artery, renal veins and duodenum.

*Urinary tract*

Using the coronal imaging technique the upper urinary tract can be demonstrated in a manner similar to standard X-ray techniques (Fig. 6) as well as being displayed in axial section (Fig. 7).

Since the kidneys are highly vascular, they have a relatively long relaxation time, which lengthens in acute nephritis and pyelonephritis. In acute tubular necrosis the organ is swollen and has a long relaxation time, allowing easy differentiation from post-renal failure. NMR may be used to display the kidneys in sections similar to those of X-ray CT scanning and to display differences in tissue character. This makes it a more accurate technique than ultrasound scan or intravenous urography in the differentiation of renal tumours from cysts, and also in a wide spectrum of renal disease. Renal cysts are usually round and smooth and contain fluid of a very long $T_1$, similar to urine. Tumours of the kidney are often irregular in shape and have relaxation values which are similar to those of normal kidney or slightly shorter (Fig. 7). If the centre of the tumour is necrotic, the $T_1$ will be lengthened, but not as much as it is for a cyst.

Infiltration of bladder tumours into the muscle have been demonstrated before any evidence of infiltration can be demonstrated with X-ray CT, these findings being subsequently confirmed by cystoscopy and biopsy. It would appear from our preliminary work that NMR will prove to be more informative than X-ray CT in the staging of bladder neoplasia.

NMR can differentiate benign prostatic hypertrophy (Fig. 8) from carcinoma of the prostate (Fig. 9). In benign hypertrophy the gland appears uniformly grey and is well encapsulated, whilst in cases of carcinoma the gland appears more granular and its outline is not as clearly defined. The relaxation time of carcinoma of the prostate is not significantly longer than that seen in benign hypertrophy. When a long relaxation time is seen it is more likely to be due to prostatitis than to malignancy.

Tumours of the testes are well demonstrated; they have relaxation times shorter than normal testis (Fig. 10) which makes for easy differentiation from cystic lesions in the scrotum, which have very long relaxation times.

The use of NMR in the evaluation of gynaecological malignancy also appears to have great promise. So far it has been our experience that it is superior to X-ray CT in the staging of cervical and uterine malignancy and no worse than it in the staging of ovarian tumours.

## CONCLUSION

Whilst experience with NMR proton imaging is still limited, it is clear that it provides a unique method for both tumour diagnosis and management. As our knowledge improves and the technique is further developed it is more than likely to replace X-ray CT as the CT method of choice for tumour imaging and staging. Furthermore, the fact that no known side-effect has been demonstrated makes it an ideal method for both repeated follow-up studies and the examination of children [6-8].

## REFERENCES

1. Pykett IL. NMR imaging in medicine. *Sci Am* 1982, **246**, 78-88.
2. Pykett IL, Newhouse JH, Buonanno FS *et al.* Principles of nuclear magnetic resonance imaging. *Radiolgy* 1982, **143**, 157-168
3. Edelstein WA, Hutchison JMS, Johnson G, Redpath TW. Spin-warp NMR Imaging and applications to human whole-body imaging. *Phys Med Biol* 1980, **25**, 751-756.

4. Edelstein WA, Hutchison JMS, Smith FW, Mallard JR, Johnson G, Redpath TW. Human whole-body NMR tomographic imaging: normal sections. *Br J Radiol* 1981, **54**, 149–151.
5. Hutchison JMS, Edelstein WA, Johnson G. A whole-body NMR imaging machine. *J Phys E: Sci Instrum* 1980, **13**, 947–955.
6. Reid A, Smith FW, Hutchison JMS. Nuclear magnetic resonance imaging and its safety implications: follow-up of 181 patients. *Br J Radiol* 1982, **55**, 784–786.
7. Smith FW. Safety of NMR imaging. *Lancet* 1982, **i**, 974.
8. Smith FW. The potential role of NMR imaging in pediatric practice. *Pediatr Radiol* 1983, **13**, 141–147.
9. Smith FW, Mallard JR, Hutchison JMS *et al.* Clinical application of nuclear magnetic resonance. *Lancet* 1981, **i**, 78–79.
10. Smith FW, Hutchison JMS, Mallard JR *et al.* Oesophageal carcinoma demonstrated by wholebody nuclear magnetic resonance imaging. *Br Med J* 1981, **282**, 510–512.
11. Smith FW, Mallard JR, Reid A, Hutchison JMS. Nuclear magnetic resonance tomographic imaging in liver disease. *Lancet* 1981, **i**, 963–966.